

# POLITECNICO DI TORINO

Collegio di Ingegneria Aerospaziale

Master of Science

**Aerospace Engineering: Propulsion Systems**



Master's Degree Thesis

## **Topology Optimization of Aeronautical Gears**

**Supervisors:**

Prof. Paolo Maggiore

.....

Ing. Luca Ronchiato

.....

Ing. Edoardo Peradotto

.....

**Candidate:**

Artero Carlo

.....

March 2018



# Ringraziamenti



# Sommario

L'ottimizzazione topologica è uno strumento matematico utilizzato per trovare un dominio in cui la distribuzione di materiale ottimizza una certa funzione obiettivo, soggetta a specifiche limitazioni. Questa tesi si pone come obiettivo lo sviluppo di una metodologia in grado di guidare il processo di ottimizzazione attraverso le tipiche limitazioni inerenti la dinamica vibrazionale delle ruote dentate. Tale metodo verrà quindi applicato a componenti rotanti atti alla trasmissione di potenza, impiegati nei moderni sistemi propulsivi aeronautici.

Lo strumento di analisi ed ottimizzazione è stato sviluppato quasi interamente all'interno dell'ambiente di lavoro OPTISTRUCT, facente parte del pacchetto di prodotti ALTAIR.

La componente più innovativa della presente tesi è costituita dal tentativo di implementazione della ciclo-simmetria nell'ottimizzatore. Tale semplificazione permetterebbe l'analisi e l'ottimizzazione a partire dal modello di un singolo settore dell'ingranaggio anziché dall'intera ruota, risparmiando così una notevole quantità di tempo CPU.

L'intero lavoro di tesi è stato svolto all'interno dell'azienda **GE AVIO S.r.l.**, in collaborazione con il **Politecnico di Torino**.



# Abstract

Topology optimization is a mathematical tool for finding a domain in which material is distributed that optimizes a certain objective function subject to specific constraints. This thesis has as its objective the development of a methodology able to guide the optimization process through the typical limitations inherent to the vibrational dynamics of the toothed wheels. This method will then be applied to rotating components suitable for power transmission, used in modern aeronautical propulsion systems.

The analysis and optimization tool has been developed almost entirely within the OPTISTRUCT work environment, which is part of the ALTAIR product package.

The most innovative component of this thesis is the attempt to implement the cyclic symmetry in the optimizer. This simplification would allow analysis and optimization from the model of a single gear sector rather than from the entire wheel, thus saving a significant amount of CPU time.

This Msc. thesis has been carried out at **GE AVIO S.r.l.** under a mutual industrial agreement between **Politecnico di Torino** and GE AVIO S.r.l.



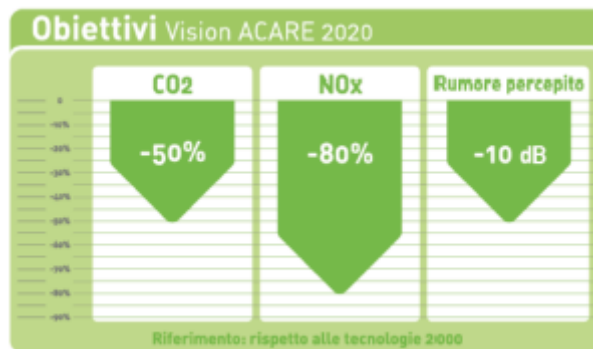
# List of Contents

<b>Sommario .....</b>	<b>5</b>
<b>Abstract .....</b>	<b>7</b>
<b>Introduction .....</b>	<b>11</b>
<b>1. Literature.....</b>	<b>13</b>
1.1 Mechanical Vibrations.....	13
1.1 Introduction on gears.....	13
1.1.1 Spur gears.....	13
1.1.2 Helical gears .....	14
1.1.3 Bevel gears .....	15
1.1.4 Worm gears.....	16
1.2 Modal Analysis theory.....	17
1.2.1 Normal modes.....	17
1.2.2 Multi-degree-of-freedom System.....	17
<b>2. Optimizations Techniques .....</b>	<b>20</b>
2.1 Topology optimization .....	21
2.2 Topology optimization in Optistruct environment.....	23
2.2.1 SIMP Method.....	24
2.2.2 BESO Method.....	25
2.3 Topology optimization for a Structural C-clip.....	26
2.3.1 Set up the Model .....	26
2.3.2 Analyze the baseline model .....	27
2.3.3 Set up the optimization problem .....	28
2.3.4 Post process the optimization results .....	28
<b>3. Cyclic Symmetry .....</b>	<b>32</b>
3.1 Cyclic symmetry equations .....	32

3.1.1	The basic sector.....	33
3.2	Duplicate sector method.....	33
3.2.1	Coupling and Constraint Equations .....	34
3.2.2	Harmonic Index and Nodal Diameter .....	35
3.3	Cyclic Symmetry in Optistruct.....	36
3.3.1	Modal analysis validation .....	39
3.3.2	Dynamic topology optimization.....	45
3.3.3	Static validation.....	47
3.3.4	Conclusions on the duplicate sector method.....	51
<b>4.</b>	<b>Test Case: GE 9X TGB PINION .....</b>	<b>51</b>

# Introduction

This thesis is part of a much wider project in which is involved a dense network of big, medium and little companies operating in the aeronautical field in Piedmont. The project, known as GREAT 2020 (Great Engine for Air Traffic 2020) was born in 2009 and has the aim to reach, within 2020, the purposes defined by the European Commission together with a group of experts ACARE (Advisory Council for Aviation Research and Innovation in Europe), concerning in a drastic reduction of polluting emissions and a greater efficiency of all the services offered to the user. The project is based on the collaboration between the enterprises present on the territory, advanced research centers and Politecnico di Torino. The company head of the project is GE AVIO AERO, leader in the research and development of aerospace propulsion system. The Politecnico di Torino inserts itself in the project GREAT 2020 as a research center, providing an occupational field in common for Politecnico researchers and Avio Aero's ones. The main objectives of the project concern in an 80 % reduction of NO<sub>x</sub> emission, a 50% reduction of the CO<sub>2</sub> emission and a reduction of the perceived noise up to 10 dB in comparison with 2000 technologies.



These purposes can be reached drastically intervening on each component of the propulsion system, the aim is to create an engine with greater efficiency and less weight. All these objectives are reachable only developing new technologies, configurations and systems, capable to move the operative limit towards more extreme conditions.



# 1. Literature

## 1.1 Mechanical Vibrations

Mechanical vibrations consist in the oscillation around a middle position of the parts which compose a specific mechanical system. Vibration's origins can be found in bodies deformability, in fact, bodies are able to storage elastic potential energy which subsequently is converted in kinetic energy and vice-versa. This continuous internal exchange of potential and kinetic energy manifests itself with vibrations around an initially equilibrium condition.

In an un-damped system, after that system has been excited, vibration continue to occur for an infinite times period, and their natural frequencies are function only of system's mass and elasticity proprieties. Instead, if in the system are present some dumpers, thanks to their relative effects, part of the mechanic energy initially introduced gets lost in each vibration life-cycle, so that vibrations decrease over time tending to disappear.

Vibration can be divided in two categories depending on the existence or not of a continuous excitation source: if it exists than they are named "forced vibration", otherwise "free vibrations".

## 1.1 Introduction on gears

### 1.1.1 Spur gears

Spur gears or straight-cut gears are the most common type of gears that can be found in mechanical applications. They have straight teeth, and are mounted on parallel shafts, for this reason, no axial thrust is created by the tooth loads. Sometimes, many spur gears are used at once to create very large gear reductions.



*Figure 0-1 Spur gear engagement*

Spur gears are used in many devices which work at moderate speeds. This is because they tend to be noisy at high speed. In fact, each time a gear tooth engages a tooth on the other gear, the teeth collide, and this impact makes a noise and increases the stress on the gear teeth.

### 1.1.2 Helical gears

Helical or "dry fixed" gears offer a refinement over spur gears. Their teeth are cut at an angle to the face of the gear. When two teeth on a helical gear system engage. The contact starts at one end of the tooth and gradually spreads as the gears rotate, until the two teeth are in full engagement.



*Figure 0-2 Helical gear engagement*

This gradual engagement makes helical gears operate much more smoothly and quietly than spur gears. For this reason, helical gears are used in almost all mechanical transmissions.

Because of the angle of the teeth on helical gears, they create a thrust load on the gear when they mesh. Therefore, devices that use this type of gears have bearings that can support this axial load, and a greater degree of sliding friction between the meshing teeth, often addressed with additives in the lubricant..



*Figure 0-3 Crossed Helical gears*

Helical gears can be meshed in parallel or crossed orientations. The former refers to when the shafts are parallel to each other; this is the most common orientation. In the latter, the shafts are non-parallel, and in this configuration the gears are sometimes known as "skew gears".

### 1.1.3 Bevel gears

A bevel gear is shaped like a right circular cone with most of its tip cut off. Bevel gears are useful when the direction of a shaft's rotation needs to be changed. They are usually mounted on shafts that are 90 degrees apart, but can be designed to work at other angles as well. The teeth on bevel gears can be straight, spiral or hypoid. Straight bevel gear teeth actually have the same problem as straight spur gear teeth: as each tooth engages, it impacts the corresponding tooth all at once.



*Figure 0-4 Straight bevel gears*

Just like spur gears, the solution to this problem is to curve the gear teeth. These spiral teeth engage just like helical teeth: the contact starts at one end and progressively spreads across the whole tooth.



*Figure 0-5 Spiral Bevel gears*

On straight and spiral bevel gears, the shafts must be perpendicular to each other, but they must also be in the same plane. If you were to extend the two shafts past the gears, they would intersect. The hypoid gear, on the other hand, can engage with axes in different planes.



*Figure 0-6 Hypoid Bevel gear*

This feature is used in many car differentials. The ring gear of the differential and the input pinion gear are both hypoid. This allows the input pinion to be mounted lower than the axis of the ring gear.

When two bevel gears mesh, their imaginary vertices must occupy the same point. Their shaft axes also intersect at this point, forming an arbitrary non-straight angle between the shafts. The angle between the shafts can be anything except zero or 180 degrees. Bevel gears with equal numbers of teeth and shaft axes at 90 degrees are called miter gears.

#### **1.1.4 Worm gears**

Worm gears are used when large gear reductions are needed. It is common for worm gears to have reductions of 20:1, and even up to 300:1 or greater.



*Figure 0-7 Worm gears*

Many worm gears have an interesting property that no other gear set has: the worm can easily turn the gear, but the gear can't turn the worm. This is because the angle on the worm is so shallow that when the gear tries to spin it, the friction between the gear and the worm holds the worm in place.

This feature is useful for machines such as conveyor systems, in which the locking feature can act as a brake for the conveyor when the motor is not turning. One other very important usage of worm gears is in the torsion differential, which is used on some high-performance cars and trucks.

## **1.2 Modal Analysis theory**

### **1.2.1 Normal modes**

Mechanical, electrical or acoustical devices are all examples of vibrating systems. They have specific oscillating patterns in which their components vibrate all at the same frequency. These patterns are called the 'normal modes' of the system. The 'natural frequencies' are the specific frequencies that corresponds to each normal mode. Generally, a physical system does not oscillate according to a single normal mode, but rather according to a combination or, better, a superposition of more of them.

A modal analysis determines the vibration characteristics (natural frequencies and mode shapes) of a structure or a machine component. It can also serve as a starting point for another, more detailed, dynamic analysis, such as a transient dynamic analysis, a harmonic analysis, or a spectrum analysis. The natural frequencies and mode shapes are important parameters in the design of a structure for dynamic loading conditions.

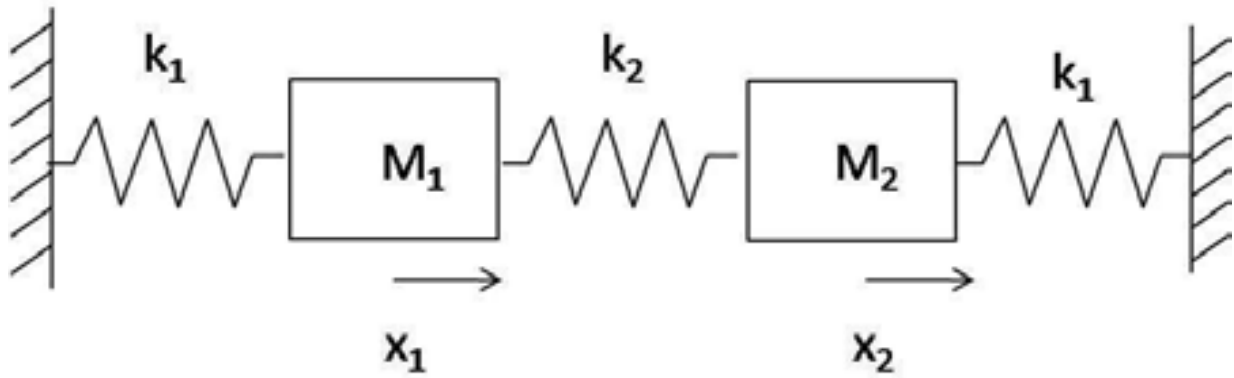
If there is damping in the structure or machine component, the system becomes a damped modal analysis. For a damped modal system, the natural frequencies and mode shapes become complex.

For a rotating structure or machine component, the gyroscopic effects resulting from rotational velocities are introduced into the modal system. These effects change the system's damping. The damping can also be changed when a Bearing is present, which is a common support used for rotating structure or machine component. The evolution of the natural frequencies with the rotational velocity can be studied with the aid of Campbell Diagram Chart Results.

### **1.2.2 Multi-degree-of-freedom System**

In this Thesis work, modal analysis has been performed on MDOF systems [5].

*Figure 1.4: System of three springs and two masses. Figure by MIT OCW*



### 1.2.2.1 Free response of Multi-degree-of-freedom System

This system has two DOF, the equations of motion in this case are:

$$m\ddot{x}_1 + k_1x_1 - k_2(x_2 - x_1) = 0 \quad (1.1)$$

$$m\ddot{x}_2 + k_2x_2 + k_2(x_2 - x_1) = 0 \quad (1.2)$$

With  $F = \begin{Bmatrix} f_1 \\ f_2 \end{Bmatrix} = \begin{Bmatrix} 0 \\ 0 \end{Bmatrix}$ .

Through matrix notation it becomes:

$$\begin{bmatrix} m & 0 \\ 0 & m \end{bmatrix} \begin{Bmatrix} \ddot{x}_1 \\ \ddot{x}_2 \end{Bmatrix} + \begin{bmatrix} k_1 + k_2 & -k_2 \\ -k_2 & k_1 + k_2 \end{bmatrix} \begin{Bmatrix} x_1 \\ x_2 \end{Bmatrix} = \begin{Bmatrix} 0 \\ 0 \end{Bmatrix} \quad (1.3)$$

It is possible to recognize:

$$M = \begin{bmatrix} m & 0 \\ 0 & m \end{bmatrix}, \text{ mass matrix}$$

$$K = \begin{bmatrix} k_1 + k_2 & -k_2 \\ -k_2 & k_1 + k_2 \end{bmatrix}, \text{ stiffness matrix}$$

$$x = \begin{Bmatrix} x_1 \\ x_2 \end{Bmatrix}, \text{ displacement vector}$$

So,

$$M \ddot{x} + Kx = 0. \quad (1.4)$$

We are looking for solution of the form:

$$\begin{Bmatrix} x_1 \\ x_2 \end{Bmatrix} = \begin{Bmatrix} c_1 \\ c_2 \end{Bmatrix} \cos(\omega t - \phi) = \begin{Bmatrix} c_1 \\ c_2 \end{Bmatrix} e^{i\omega t} \quad (1.5)$$

The condition that needs to be verified is:

$$([K] - \omega^2[M])\{X\}e^{i\omega t} = \{0\} \quad (1.6)$$

For which non-trivial solution are those which satisfy:

$$\det|[K] - \omega^2[M]| = 0 \quad (1.7)$$

A general solution for the equation can be expressed in the form:

$$\begin{Bmatrix} x_1 \\ x_2 \end{Bmatrix} = A \begin{Bmatrix} 1 \\ 1 \end{Bmatrix} e^{i\omega_1 t} + B \begin{Bmatrix} 1 \\ -1 \end{Bmatrix} e^{i\omega_2 t} \quad (1.8)$$

Where: A, B,  $\omega_1$ ,  $\omega_2$  are determined by initial conditions.

In order to satisfy condition expressed in equation (1.7) for a N-DOF system, N values of  $\omega^2$  can be found, which represent the natural frequencies of the un-damped system.

Substituting each frequency into equation (1.6) it is possible to calculate the vector  $\{X\}$  for each of them, this is called also mode shape  $\{\Phi\}_r$ , which represent the relative displacements of all parts of the system for the  $r^{\text{th}}$  natural frequency.

Thus, the complete solution can be expressed in two N x N matrices, called the eigenmatrices,

- $[\cdot \bar{\omega}_r^2 \cdot] \rightarrow \text{Natural frequencies}$
- $[\Psi] \rightarrow \text{Mode shapes}$

### 1.2.2.2 Orthogonality properties

Before introducing damping in MDOF system, it is important to remember the orthogonality property of modal matrices. This consist in:

- $[\Psi]^T [K] [\Psi] = [k_r]$
- $[\Psi]^T [M] [\Psi] = [m_r]$

From which  $[\bar{\omega}_r^2] = [m_r]^{-1} [k_r]$  where  $m_r$  and  $k_r$  are often referred to as the modal mass and modal stiffness of mode r.

### 1.2.2.3 MDOF system with proportional damping

The main advantage of using a proportional damping model in structural analysis is that the modes are almost identical to those ones of the un-damped model. Specifically, the mode shapes are identical and the natural frequencies are very similar to those ones of the un-damped system. In fact, it is possible to obtain modal properties of a proportionally-damped system by analyzing the un-damped model and then correcting it considering the presence of damping.

With reference to the equation (1.4), adding the damping term, it is obtained:

$$[M]\{\ddot{x}\} + [C]\{\dot{x}\} + [K]\{x\} = \{f\} \quad (1.9)$$

Considering the case in which the damping is directly proportional to the stiffness:

$$[C] = \beta[K]$$

In this case, it is clear that if we pre- and post- multiply the damping matrix by the eigenvector matrix for the un-damped system,  $[\Psi]$ , in just the same way as was done for the mass and stiffness matrices, then we shall find:

$$[\Psi]^T [C] [\Psi] = \beta [k_r] = [c_r]$$

where the diagonal elements,  $c_r$ , represent the modal damping of the various modes of the system. The fact that this matrix is also diagonal means that the un-damped system mode shapes are also those of the damped system, and this is a particular feature of this type of damping. This statement can easily be demonstrated by taking the general equation of motion above (1.8) and, for the case of no excitation, pre- and post- multiplying the whole equation by the eigenvector matrix,  $[\Psi]$ . We shall then find

$$[m_r]\{\ddot{p}\} + [c_r]\{\dot{p}\} + [k_r]\{p\} = \{0\} \quad \text{where} \quad \{p\} = [\Psi]^{-1}\{x\} \quad (1.10)$$

from which the  $r^{\text{th}}$  individual equation is:

$$m_r \ddot{p}_r + c_r \dot{p}_r + k_r p_r = 0 \quad (1.11)$$

which is clearly that of a single-degree-of-freedom system, or of a single mode of the system. This mode has a complex natural frequency with an imaginary (oscillatory) part:

$$\omega_r' = \bar{\omega}_r \sqrt{1 - \zeta_r^2} \quad ; \quad \bar{\omega}_r^2 = \frac{k_r}{m_r} \quad ; \quad \zeta_r = \frac{c_r}{2\sqrt{k_r m_r}} = \frac{1}{2} \beta \bar{\omega}_r$$

and a real (decay) part:

$$a_r = \zeta_r \bar{\omega}_r = \frac{\beta}{2}$$

These characteristics carry over to the forced response leads to the definition of the general receptance FRF as:

$$[\alpha(\omega)] = [K + i\omega C - \omega^2 M]^{-1} \quad (1.12)$$

Or:

$$\alpha_{jk}(\omega) = \sum_{r=1}^N \frac{(\psi_{jr})(\psi_{kr})}{(k_r - \omega^2 m_r) + i(\omega c_r)}$$

## 2. Optimizations Techniques

The reduction of vibration and noise is one of the main issue in gear design. The noise generated by gears is mainly due to the transmission error fluctuation, which is the difference between the theoretical relative position of two unloaded gears (without manufacturing errors) and the relative position of a gear pair under actual operating conditions.

Introducing suitable geometry modification allows to change the frequency response of a gear in terms of amplitude and phase.

Literature offers many approaches to evaluate the dynamic behavior of such systems and their design optimization. In the last century, optimization approaches were mainly based on simplified analytical model. In the last years were presented a lot of different optimization method for gears dynamics, the majority of which focused on micro-geometrical modifications of the teeth profile of the gear, by using a wide variety of optimization methodologies.

There are a lot of different optimizations techniques which can be grouped in to two big families: structural optimizations and dimensional optimization.

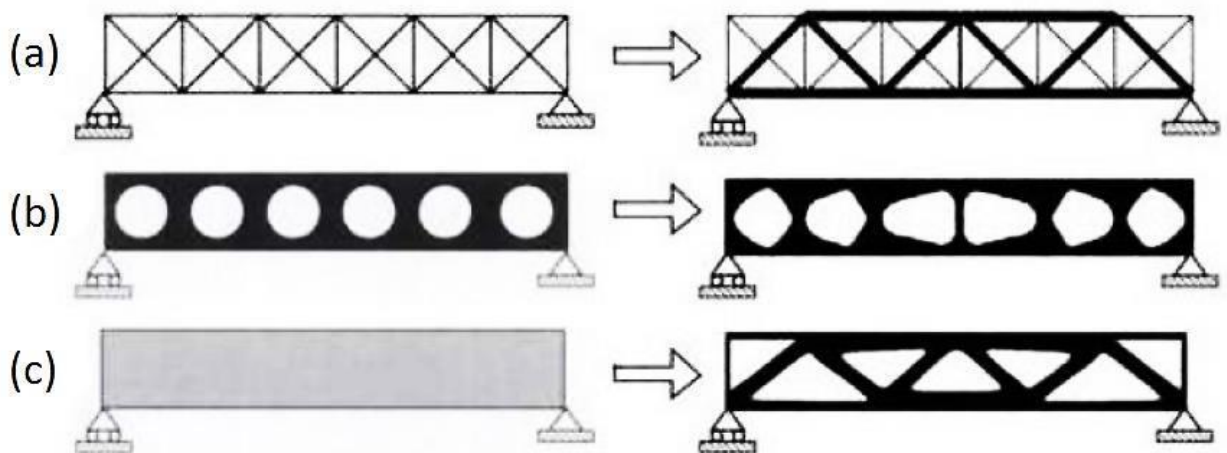
In the dimensional optimization family there are two techniques:

- **Shape Optimization:** In order to achieve the desired performance values of the object, the algorithm modifies the shape parameters according to the boundary conditions; the calculation variables are therefore: radius, fittings, chamfers, thicknesses, characteristic dimensions, etc;

- **Size Optimization:** used for the calculation of structures defined through the use of one-dimensional or at most two-dimensional elements; the optimal characteristic values of these elements are calculated in order to achieve the objective imposed by the user according to the boundary conditions. The parameters used can be thickness, properties of the 1D and 2D elements, properties of the materials, etc;

Based on the structural approach there are the following optimization techniques:

- **Topology Optimization:** used to define the preliminary design of a component. It is based on algorithms for the calculation of the optimal density distribution within a calculation domain in compliance with the boundary conditions imposed by the user;
- **Topography optimization:** this optimization technique is very often used on two-dimensional objects, on which, once discretized by finite elements, the ribs and the necessary ridges are calculated in order to satisfy the user's performance requirements according to the imposed boundary conditions;
- **Topometry Optimization:** this optimization method is basically a dimensional optimization made element by element: in fact during the optimization the characteristic parameter (thickness, parameters of the 1D elements, etc.) of each single element is changed until the target is achieved. Shape optimization is distinguished from topometry by the fact that the elements are grouped into distinct computational domains in which the properties must be constant, therefore the shape optimization does not take place element by element but domain by domain.



## 2.1 Topology optimization

During the process of improvement or creation of a new product, one of the most complex and decisive step is to define the component geometry. This is obtained, as a first approximation, thanks to the experience of the designers. In fact, from the knowledge of the boundary conditions and the necessary interfaces, they are able to generate a first attempt model. The geometry thus created is optimized by means of an iterative methodology that involves static, dynamic and fatigue analysis, which allow the identification of the final shape that the component must possess in respect of the imposed design constraints. Since all the sizing analysis take place on the first attempt model, it is fundamental to use a method to obtain the best possible geometry in order to obtain an efficiently and quickly component with an optimal shape. In this regard, the structural optimization technology is considered, which was designed both to reduce the design time and to obtain the best possible performance from the components subjected to this process.

Topology optimization is a process for which, defined a geometric domain and its boundary conditions, obtains the optimal density distribution according to a goal defined by the designer and a series of constraints imposed to guarantee the functionality of the component. The use of these processes turns out to be crucial both in the design phase from scratch, and in the case in which the performance of an existing object is to be increased. In fact they allow not only to drastically reduce design time but also to obtain much better results than those obtainable thanks to conventional design methods.

First of all, topology optimization requires the definition of a geometric domain on which the calculation will be performed, this geometry must be discretized through the use of finite elements. Subsequently the boundary conditions and the properties of the material will be defined (modulus of elasticity, density and Poisson coefficient). Once the forces and constraints are entered in the model, the optimization parameters will be defined (maximum nodal shift, maximum allowed voltage value, value of the first own frequency, etc.) and finally the optimization target will be defined, as for example minimize mass, maximize stiffness, etc.

In literature there are a multiplicity of methods to solve the problem mentioned above, these are grouped into two distinct families, depending on the calculation approach used:

- **Microstructural approach:** the variables to the problem are the elastic properties of the material, which are correlated, through appropriate functions, to the normalized density of the single element. The final result will be defined by a geometry identical to the initial one, where however each element will be assigned a normalized density between zero and one: the first value corresponds to the elements that will have to be removed, as they are not useful for the problem; while those with a unit density value are the elements that will have to describe the new geometry. Then there will be a certain quantity of elements with intermediate density at the two extreme values: the calculation algorithm suggests that those are elements that have a lower degree of 'importance' for the structure but that in any case can't be neglected. It is therefore necessary to attribute a physical interpretation, so as to be able to discriminate their actual usefulness and verify if the solution is realizable or not. There are two schools of thought: the first is that according to which these elements must be eliminated in favor of those with a zero or unitary density value, in order to define in a clear and precise way the optimized geometry; the second exploits this distribution of intermediate densities to give those zones a certain degree of porosity to the material or the insertion of inserts in different materials.
- **Macrostructural approach:** the calculation variable is the very geometry of the component, in fact during the iterations, the algorithm modifies the size and the number of elements that describe the computational domain, which is optimized in compliance with the imposed geometric constraints; there is therefore no presence of intermediate densities.

The first approach turns out to be the most widespread since it is the most robust and simple to implement in calculation software, furthermore it has the advantage of being able to use anisotropic materials and a calculation domain of any shape. On the contrary, the macrostructural approach requires a well-defined starting geometry in order to obtain satisfactory results, for this reason this approach is mostly used for optimizations of existing structures and not for the generation of new geometries. [reference?]-vedi cucco 13 16 17]

## **2.2 Topology optimization in Optistruct environment**

Topology Optimization is a mathematical technique that produces an optimized shape and material distribution for a structure within a given package space. By discretizing the domain into a finite element mesh, OptiStruct calculates material properties for each element. The OptiStruct algorithm alters the material distribution to optimize the user-defined objective under given constraints.

The topology optimization technique yields a new design and optimal material distribution. Topology optimization allows designers to start with a design that already has the advantage of optimal material distribution and is ready for design fine tuning with shape or size optimization. In literature there are many methods for solving optimization problems. The most common are the SIMP and BESO: the first is the most used approach by commercial software including Altair Optistruct, used for this thesis; the second one is still under development and its implementation in the immediate future can't be ruled out.

## 2.2.1 SIMP Method

The equations that govern the calculation of topological optimization are based on energetic principles derived from Eschenauer, Olhoff and Schnell.

The mathematical model, with a microstructural approach, typically used by commercial programs, is the S.I.M.P. (Solid Isotropic Material with Penalization) which results to have a discrete formulation with a relaxation function; the calculation is carried out in an iterative manner.

$$\min: F_{obj} = \sum_{i=1}^N \rho(x)^p u_i K_i u_i \quad 0 \leq \rho_i \leq 1$$

$$E(x) = \rho(x)^p \cdot E_0 \quad p > 1$$

The equation 2.1 is the mathematical expression of the topological optimization problem:

- **$\rho(\mathbf{x})$** : is the normalized density distribution associated to the calculation domain, called the design space or the design domain;
- **$\mathbf{K}_i$** : is the stiffness matrix of the  $i$ -th element
- **$\mathbf{F}_{obj}$** : is the objective function, which is generally either maximized or minimized, depending on the purpose of the optimization; (in this specific case the yielding of the system is minimized)
- **$P$** : is the penalization factor;

Equation 2.2 is the penalty function where the density of the element  $\rho(x)$  is put in correlation with the stiffness matrix of the same; this allows to assign a new stiffness value to the element, note its density. The relation between mass and mechanical properties does not have a real physical meaning, but turns out to be an assumption necessary for the purposes of the calculation.

The exponent  $p$  is called 'penalty factor', this parameter is used to define the penalty curve to be used in the calculation, it allows the user to define how the density distribution should tend to extreme values, which will therefore strongly influence the validity and the form of the solution.

It is therefore of fundamental importance to insert appropriate values of the penalty factor in order to:

- **Limit the checkerboard problem**: that is the generation of geometries composed of an alternation of elements with a null and non-zero rho value, which do not allow the identification of a well-defined geometry. These density transition discontinuities cause the presence of unlinked and isolated elements, connected by a single node or interrupted geometries; forms that make the solution in fact unusable.
- **Force normalized density to extreme values**: it allows to obtain a solution in which the greatest possible number of elements have zero or unitary normalized density; it is impossible not to obtain elements with intermediate values, but with appropriate techniques [?] it is possible to considerably limit their number.

In order to obtain the above-mentioned effects,  $p$  must always be greater than 1. The resolutive scheme of the SIMP method is described by the following steps [??]:

- I. Choice of an appropriate calculation domain and implementation of body loads and constraints;
- II. Definition within the domain of the areas that must have  $\rho = 1$ , generally identified as the interfaces with other components, they will be part of the computational domain, but will always have unitary rho;
- III. Discretization of the computational domain;

- IV. Material properties definition;
- V. Nodal displacement calculation through Finished Element Method;
- VI. Calculation of the impact of the variation in density of each element with respect to the objective function, defined as the derivative of the objective function with respect to  $\rho$ . If this value is less than the imposed threshold, then the iterative process is terminated, otherwise the procedure can continue. This passage is also called sensitivity analysis;
- VII. Updating the variable  $\rho$  calculated by means of the relaxation function, this step is generally coupled with the filtering of the sensitivity in order to limit the checkerboard effect;
- VIII. Repeat iteratively the operations V, VI and VII, until the convergence is reached;
- IX. Graphical representation of the density distribution obtained.

### 2.2.2 BESO Method

BESO (Bi-directional Evolutionary Structural Optimization) is a topological optimization method based on finite element discretization belonging to the macrostructural family. The algorithm was developed to improve results and decrease the convergence time of AESO (Additive Evolutionary Structural Optimization) and ESO (Evolutionary Structural Optimization) methods. Subsequently, an improved version of the BESO method was presented for the solution of elastic deformation energy problems, which is found in the most modern texts in the literature. The methodology used to find the solution is to add useful elements (active elements) and simultaneously eliminate those that are not considered fundamental for the structure (inactive elements). In particular, the BESO method has the peculiarity that once an element is deactivated, in subsequent iterations it is possible that it is brought back to the active state if it is deemed necessary, this is a considerable advantage compared to the ESO and AESO methodologies.

The main control parameters of the algorithm are two:

- **Evolutionary Ratio (ER):** it is the rate of variation of material allowed to the design volume for each iteration;
- **Filtering radius (FR):** this is the limit distance for the calculation of average sensitivity on adjacent nodes;

The methodology with which elements are activated or deactivated is based on sensitivity analysis: for each active element this value is calculated on the base of the static analysis performed at each iteration, this takes place as a function of the displacement of the nodes belonging to the element. For all the deactivated elements, since they do not take part in the static analysis, the sensitivity factor is calculated by exploiting the nodal displacements of the elements that surround them. Once the sensitivity calculation is performed, a classification of these values from highest to lowest is carried out to allow filtering. In this part of the algorithm two sensitivity threshold values are implemented, if an element is above the upper limit it is made active, if lower than the lower limit it is deactivated. Deactivation can be done in two ways: the first one called 'soft-kill' consists in multiplying the stiffness matrix of the element by a value of  $1 \cdot 10^{-12}$ , in the second one called 'hard-kill', the element's stiffness contribution is completely eliminated. The calculation is concluded when the variation of elemental sensitivity for the  $i$ -th iteration is lower than an imposed value and if the volume fraction present at the same iteration is equal to or less than the imposed target value. Also, this method suffers from the problem of checkerboard and above all with the hard-kill method the convergence to the solution can be difficult.

## 2.3 Topology optimization for a Structural C-clip

The present chapter contains a simple topology optimization problem which is taken from the Altair Optistruct Tutorial manual [reference??]. In this example, topology optimization is performed on a model to create a new topology for the structure, removing any unnecessary material. The resulting structure is lighter and satisfies all the following design constraints:

- **Objective:** Minimize volume fraction.
- **Constraints:** Translation in the y-axis for node A < 0.07 mm.  
Translation in the y axis for node B > -0.07 mm.
- **Design Variables:** The density of each element in the design space.

In orders to achieve the optimized C-clip is necessary study in deep the following steps:

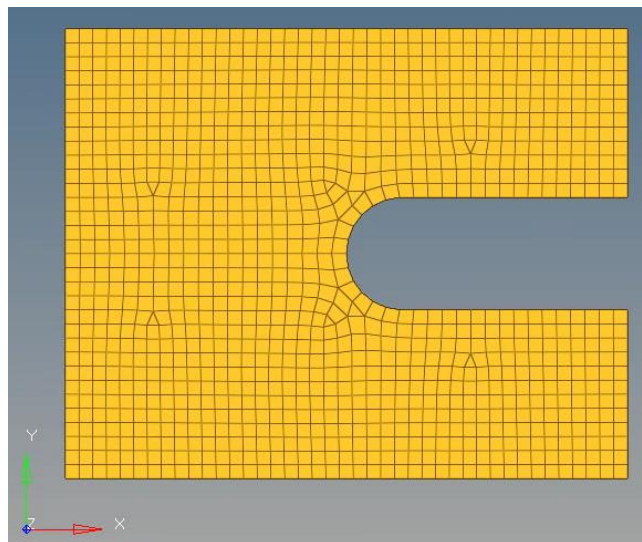
1. Set up the model in HyperMesh environment.
2. Analyze the baseline model.
3. Set up the optimization problem.
4. Post-process the optimization results.

### 2.3.1 Set up the Model

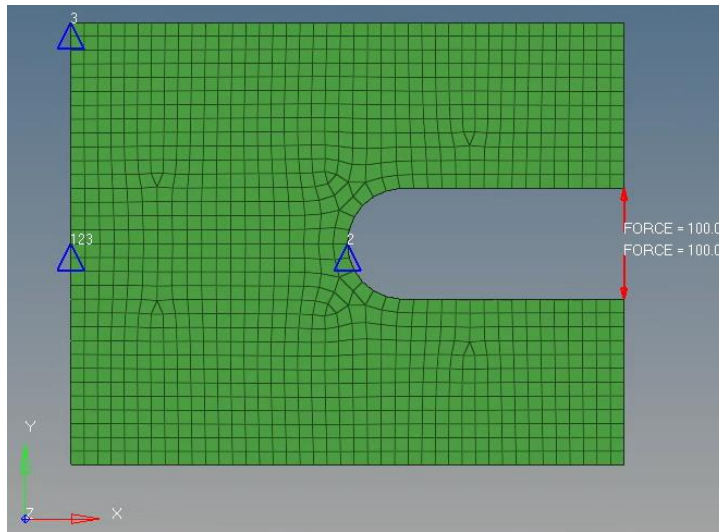
We start form the following 2D mesh model:

In orders to perform the analysis are necessary the following phases:

- a) Create Material
- b) Create PSHELL property
- c) Assign the property to the component
- d) Create forces
- e) Create constraints (SPC)



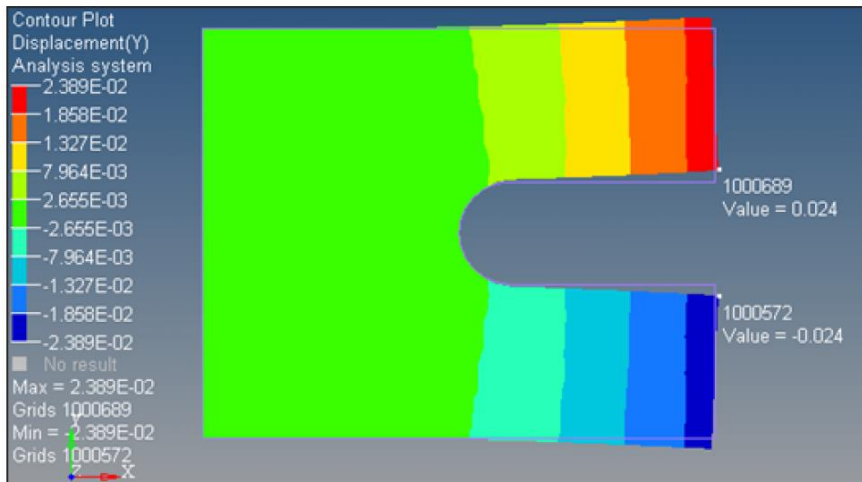
At this point we have the following baseline model:



### 2.3.2 Analyze the baseline model

A linear static analysis of this C-clip is performed prior to the definition of the optimization process. An analysis identifies the responses of the structure before optimization to ensure that constraints defined for the optimization are reasonable.

Optistruct shows the following results:



This shows the contour of the nodal displacements along the Y-axis. The forces in the structure are applied on the outer nodes of the opening of the clip, making those two nodes critical locations in the mesh where the maximum displacement is likely to occur.

In this example, we will apply a displacement constraint on these nodes so that they would not displace more than 0.07 in the y-axis.

### 2.3.3 Set up the optimization problem

The finite element model, consisting of shell elements, element properties, material properties, and loads and boundary conditions has been defined. Now a topology optimization will be performed with the goal of minimizing the amount of material to be used. Typically, removing the material in an existing volume, with the same loads and boundary conditions, makes the model less stiff and more prone to deformation. Therefore, you need to track the displacements (which represent the stiffness of the structure) and constrain the optimization process such that the least material necessary is used and overall stiffness is also achieved.

In this specific case, to set up the optimization problem we need to:

- a) Create the topology design variables
- b) Create a volume response
- c) Create a displacement response
- d) Create constraints on displacement responses
- e) Define the objective function
- f) Run Optistruct for the optimization

The message following message appears in the window at the completion of the job:

OPTIMIZATION HAS CONVERGED.  
FEASIBLE DESIGN (ALL CONSTRAINTS SATISFIED).

OptiStruct also reports error messages if any exist.

### 2.3.4 Post process the optimization results

Optistruct provides element density information for all iterations, and also gives displacement and von Mises stress results (linear static analysis) for the starting and last iterations. We are able to see these results in HyperView:

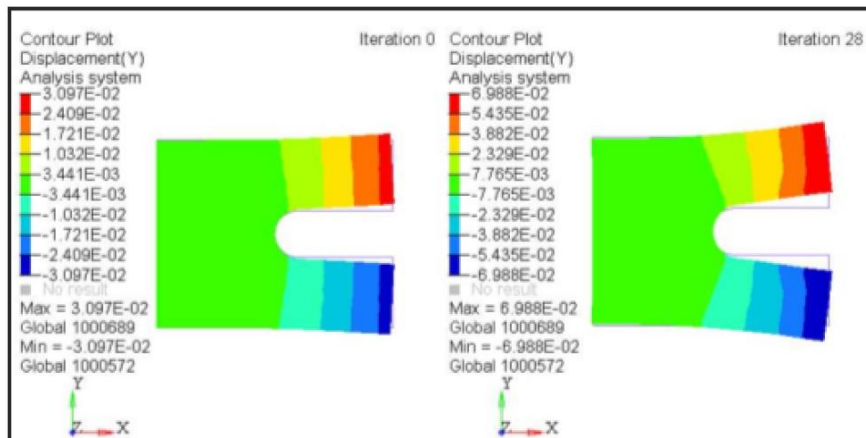
- **Iso Value Plot of Element Densities:**



This plot provides the information about the element density. Iso Value retains all of the elements at and above a certain density threshold.

Pick the density threshold providing the structure that suits our needs.

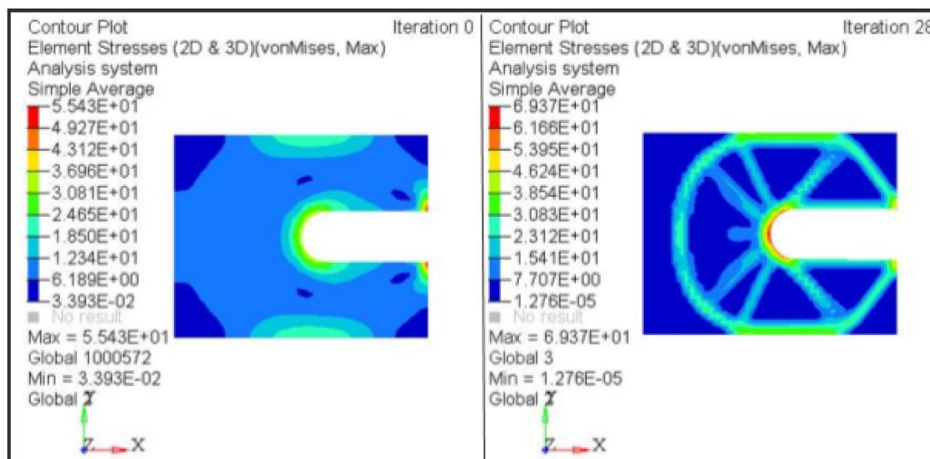
You will see the Iso value in the graphics window update interactively when you scroll to a new value. Use this tool to get a better look at the material layout and the load paths from OptiStruct.



- **Compare Static Contour of Original to the Optimized Material Layout**

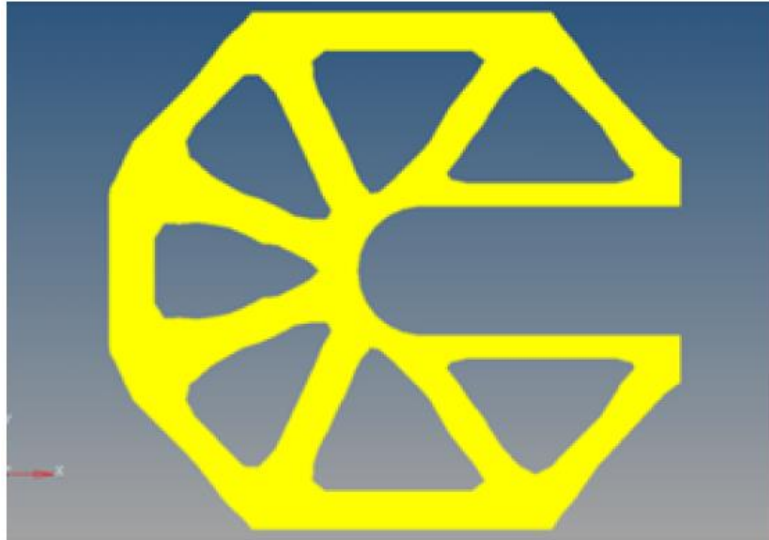
This plot provides the information about the nodal displacements of the original component (iteration 0) with those of the optimized c-clip (iteration 28):

The following stress results can be used only as reference to help understanding how far from the limits the design is. Remember that topologic optimization will show you a concept shape and the stress results should be validated during the next design phases.



Performing topology optimizations early in the conceptual design stage results in the generation of a good baseline design and contributes to a shorter design cycle. One challenge with post-processing topology optimization results is that the results may have several intermediate density elements or checkerboard patterns which can be interpreted either as solid members or as a void. If these semi-dense elements are interpreted as thin members, the final design is harder to manufacture.

OptiStruct offers the minimum member size control method which provides some control over member size in the final topology designs by defining the least dimension required in the final design. It helps achieve a discrete solution by eliminating the intermediate density elements and checkerboard density pattern, resulting in a discrete and better reinforced structure, which is easier to interpret and easier to manufacture.

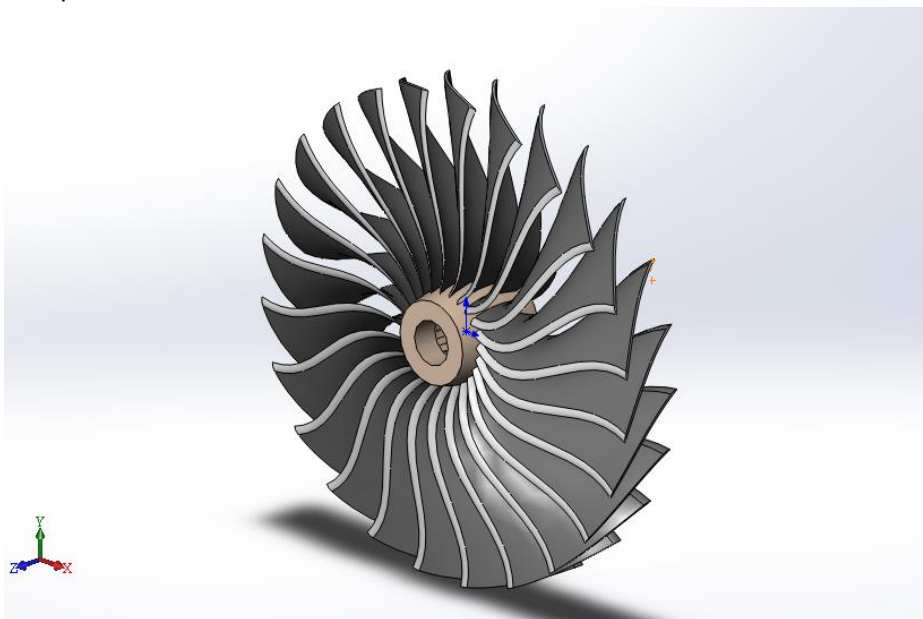


Compare this image to the one you achieved in the previous optimization without the application of minimum member size control. The iso value plot displayed is similar to the one previously. Notice the smaller members in the original iso surface plot are replaced by a more discrete rib pattern. This design is easier to manufacture.



## 3. Cyclic Symmetry

Cyclic symmetry modeling is an analysis tool used to simulate structures having a repetitive geometric pattern in 360 degrees around an axis of symmetry. Common examples of cyclically symmetric structures are turbine blade disks, gears and fans. If a structure exhibits cyclic symmetry, you can perform an automated static, modal, harmonic, or buckling analysis. Taking advantage of the repeatable geometry, a cyclic symmetry analysis can vastly reduce model size and computational cost, in fact a cyclic symmetry analysis conserves time and CPU resources and allows you to view analysis results on the entire structure. The main idea is to solve the behavior of a single symmetric sector and then use the single sector solution to construct the response of the full 360° model.



Our goal is to implement in the Optistruct environment the cyclic symmetry equations in order to perform a topology optimization of a single sector of our gear instead of the full 360° model. In the next sections we'll introduce the general cyclic symmetry equations and the duplicate sector method used to achieve our objective.

### 3.1 Cyclic symmetry equations

From the general dynamic equation:

$$[M]\{\ddot{U}\} + [C]\{\dot{U}\} + [K]\{U\} = \{f\}$$

where:

- [M] is the mass matrix;
- [C] is the damping matrix;
- [K] is the stiffness matrix;
- {U} is the solution vector;
- {f} is the external force vector;

A Fourier decomposition of the external load and the solution vector is performed:

$$\{U\} = [T]\{u_p\}$$

$$\{F\} = [T]\{f_p\}$$

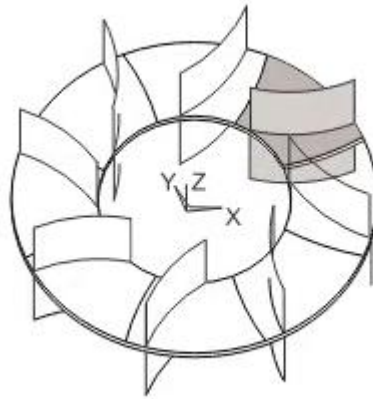
Where we introduced the transformation matrix [T] and the harmonic indices displacements and load quantities  $\{u_p\}$  and  $\{f_p\}$ . Substituting in the general dynamic equation it reduces to:

$$[T^*]^T [M] [T] \{\ddot{u}_p\} + [T^*]^T [C] [T] \{\dot{u}_p\} + [T^*]^T [K] [T] \{u_p\} = [T^*]^T [T] \{f_p\}$$

This set of uncoupled cyclic sector equations is solved while enforcing the compatibility boundary conditions between the sectors.

### 3.1.1 The basic sector

A cyclic symmetry analysis requires that you model a single sector, called the basic sector. A proper basic sector represents one part of a pattern that, if repeated N times in cylindrical coordinate space, yields the complete model:



The angle  $\alpha$  (in degrees) spanned by the basic sector should be such that:

$$N \cdot \alpha = 360$$

where N is an integer.

The basic sector can consist of meshed or unmeshed geometry.

### 3.2 Duplicate sector method

Generally, in orders to impose the cyclic symmetry to a sector, we have to implement the following relation to each element of the basic sector's faces:

$$\{q_r\} = \{q_l\} e^{-i\varphi}$$

$$\varphi = \frac{2\pi}{Z} ND$$

Where  $\{q_r\}$  and  $\{q_l\}$  are the right and left nodal displacement vectors, while  $\varphi$  is the phase angle which is function of the number of teeth and the Nodal Diameter.

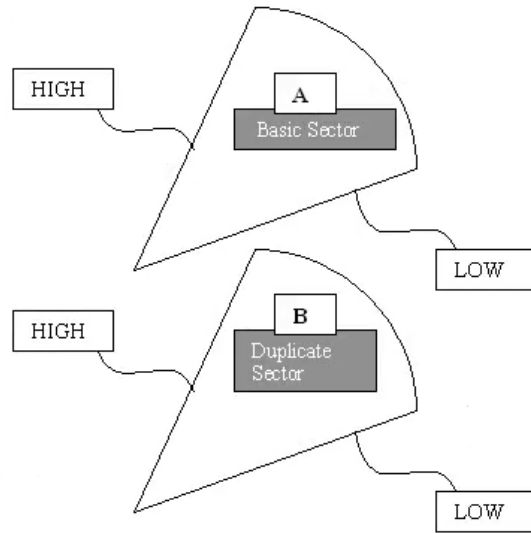
This will bring to a complex equation which can't be implemented in the Optistruct environment so we were forced to choose another way to impose the cyclic symmetry condition to the basic sector. The architecture of the cyclic symmetry solution process depends upon how the compatibility and equilibrium conditions of the cyclic sector are enforced in the matrix-solution process. The two most common solution methods are Duplicate Sector and Complex Hermitian. We chose to follow the approach suggested by Ansys which is the Duplicate Sector method.

In Ansys, during the solution stage, the program generates a duplicate sector of elements at the same geometric location as the basic sector. (Duplicate sector creation occurs automatically and transparently in

Ansys while in the Optistruct environment we had to manually create the duplicate sector model as will show later in this document.) The program applies all loading, boundary conditions, and coupling and constraint equations present on the basic sector to the duplicate sector.

### 3.2.1 Coupling and Constraint Equations

The program enforces cyclic symmetry compatibility conditions for each harmonic index solution via coupling and/or constraint equations (CEs) connecting the nodes on the low- and high-edge components on the basic and duplicate sectors.



$$\begin{Bmatrix} U_{high}^A \\ U_{high}^B \end{Bmatrix} = \begin{bmatrix} \cos(k * \alpha) & -\sin(k * \alpha) \\ \sin(k * \alpha) & \cos(k * \alpha) \end{bmatrix} \begin{Bmatrix} U_{low}^A \\ U_{low}^B \end{Bmatrix}$$

Where:

k= Harmonic index

$$k = \begin{cases} 0,1,2, \dots, N/2 & \text{when } N \text{ is even} \\ 0,1,2, \dots, \frac{N-1}{2} & \text{when } N \text{ is odd} \end{cases}$$

(N is an integer representing the number of sectors in 360°.)

$\alpha$ = Sector angle  $\frac{2\pi}{N}$

U= Vector of displacement and rotational degrees of freedom

$U_{low}^A$  represents the basic sector low side edge

$U_{high}^A$  represents the basic sector high side edge

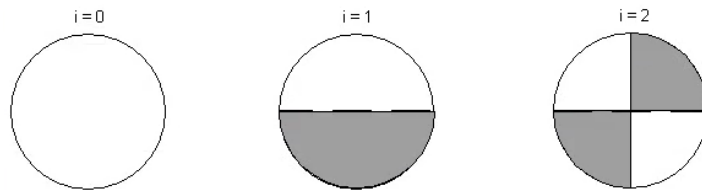
$U_{low}^B$  represents the duplicate sector low side edge

$U_{high}^B$  represents the duplicate sector high side edge

In Ansys, the last equation is a function of harmonic index  $k$  generating different sets of constraint equations for each harmonic index. Therefore, for each harmonic index solution requested, the program creates the appropriate constraint equations automatically, connects the edge-component nodes on basic sector A and duplicate sector B, and solves.

### 3.2.2 Harmonic Index and Nodal Diameter

To better understand the process involved in the following modal cyclic symmetry analysis, it is necessary to understand the concepts of harmonic indices and nodal diameters. The nodal diameter refers to the appearance of a simple geometry vibrating in a certain mode. Most mode shapes contain lines of zero out-of-plane displacement which cross the entire geometry:



It's important to remember that these zero-displacement lines are present only in structures exhibiting cyclic symmetry like gear wheels or turbine disks, however for complicated cyclic symmetric structures, nodal diameters may not be observable in a mode shape.

The harmonic index is strictly correlated to the nodal diameters. It consists in an integer that determines the variation in the value of a single degree of freedom (DOF) at points spaced at a circumferential angle equal to the sector angle. For a harmonic index equal to nodal diameter  $d$ , the following function describes the variation:

$$\cos(d \cdot \theta)$$

This definition allows a varying number of waves to exist around the circumference for a given harmonic index, provided that the DOF at points separated by the sector angle vary according to the relation above. For example, a harmonic index of 0 and a 60° sector angle produce modes with 0, 6, 12, ..., 6N waves around the circumference. The nodal diameter is the same as the harmonic index in only some cases. The solution of a given harmonic index may contain modes of more than one nodal diameter. The relationship between the harmonic index  $k$  and nodal diameter  $d$ , for a cyclic symmetric component consisting of  $N$  sectors, is reported as follow:

$$d = m \cdot N \pm k$$

Where  $m = 0, 1, 2, 3, \dots, \infty$

For instance, if a model is composed by seven sectors ( $N=7$ ) and the specified harmonic index is  $k=2$ , there will be solutions for nodal diameters 2, 5, 9, 12, 16, 19, 23, ...

A summary is reported in the following table, which illustrates how the harmonic index, number of sectors and nodal diameters relate to one another:

Harmonic Index ( $k$ )	Nodal Diameter ( $d$ )					
	0	$N$	$N$	$2N$	$2N$	...
0	0	$N$	$N$	$2N$	$2N$	...
1	1	$N-1$	$N+1$	$2N-1$	$2N+1$	...
2	2	$N-2$	$N+2$	$2N-2$	$2N+2$	...
3	3	$N-3$	$N+3$	$2N-3$	$2N+3$	...
4	4	$N-4$	$N+4$	$2N-4$	$2N+4$	...
...	...	...	...	...	...	...
$N/2$ ( $N$ is even)	$N/2$	$N/2$	$3N/2$	$3N/2$	$5N/2$	...
$(N-1)/2$ ( $N$ is odd)	$(N-1)/2$	$(N+1)/2$	$(3N-1)/2$	$(3N+1)/2$	$(5N-1)/2$	...

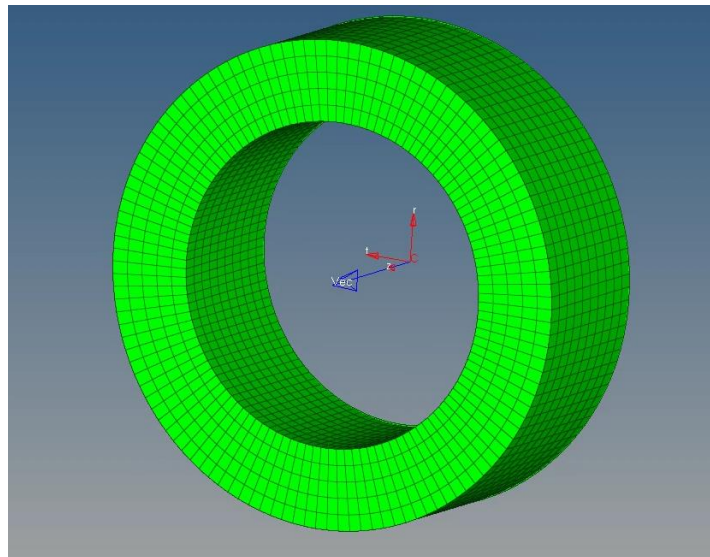
### 3.3 Cyclic Symmetry in Optistruct

The objective of this chapter is to list the procedure used to implement the duplicate sector method in the Optistruct environment.

Let's start again from the compatibility equation of the cyclic symmetry discussed above:

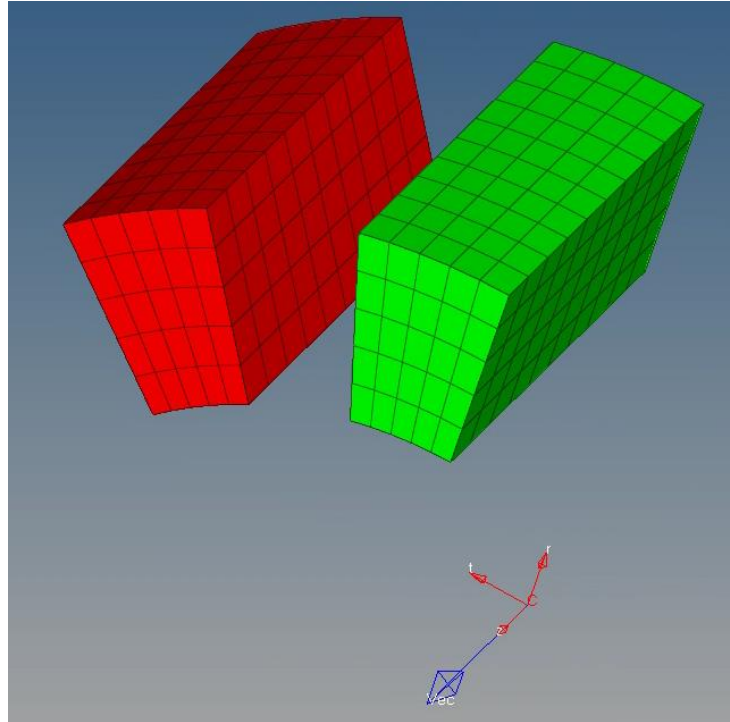
$$\begin{Bmatrix} U_{high}^A \\ U_{high}^B \end{Bmatrix} = \begin{bmatrix} \cos(k * \alpha) & -\sin(k * \alpha) \\ \sin(k * \alpha) & \cos(k * \alpha) \end{bmatrix} \begin{Bmatrix} U_{low}^A \\ U_{low}^B \end{Bmatrix}$$

In order to impose the equations at the nodes we will have to model the base sector and then duplicate it. For these purposes we chose to consider a very simple geometry which consists in a hollow cylindrical section as shown below:



The finite element model shown has been created from a flat rectangular section, meshed with 2D elements and revolutionized around the z axis of a set of cylindrical axes. Strictly speaking, this component is axially symmetric, so to impose cyclo-symmetry it is necessary to choose an arbitrary number of sectors. For these examples we choose 24 sectors each of 15 degrees.

Then proceed to modeling the base sector and the duplicate sector. In order to obtain results comparable to each other in the subsequent validation phases, it is necessary to model the sectors maintaining the same mesh of the initial component. Otherwise we would certainly get different results that could influence our judgment on the goodness of the method.



From now on we'll consider the green sector as the basic sector and the red one as the duplicated sector or in other words the real and the imaginary parts of a single sector of the cyclic symmetric structure. In fact don't make the mistake to think at those sectors like two separated entities but always remember that they are representing only one single sector of the initial model.

At this point we can proceed with the implementation of the equations in the Optistruct environment through the definition of the appropriate multi point constraints (MPC). To apply the duplicate sector method we chose to manually modify the solver deck file created by Hypermesh (.fem extension) to impose the correct MPC weights. Let's see the following example considering a nodal diameter equal at 2:

- $ND = 2;$
- $\alpha = 15^\circ;$
- *Radial displacement considered at nodes: 10000 20056 30000 40056*

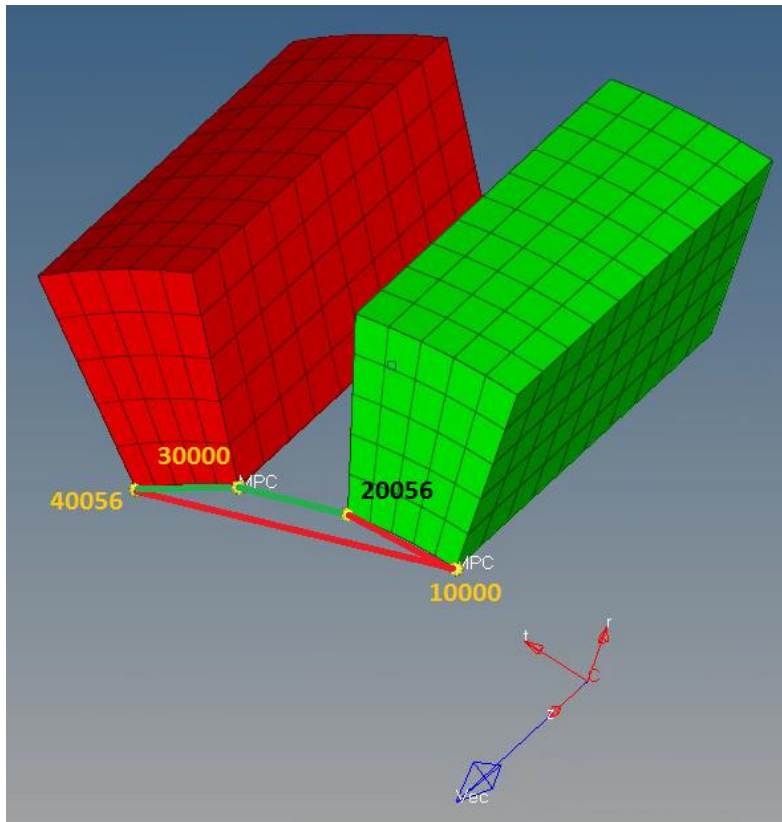
$$-x_{10000} + \cos(2 * 15^\circ) * x_{20056} + \sin(2 * 15^\circ) * x_{40056} = 0$$

MPC	3	10000	1-1.0	20056	1.8660254	+
+		40056	10.5			

$$-x_{30000} - \sin(2 * 15^\circ) * x_{20056} + \cos(2 * 15^\circ) * x_{40056} = 0$$

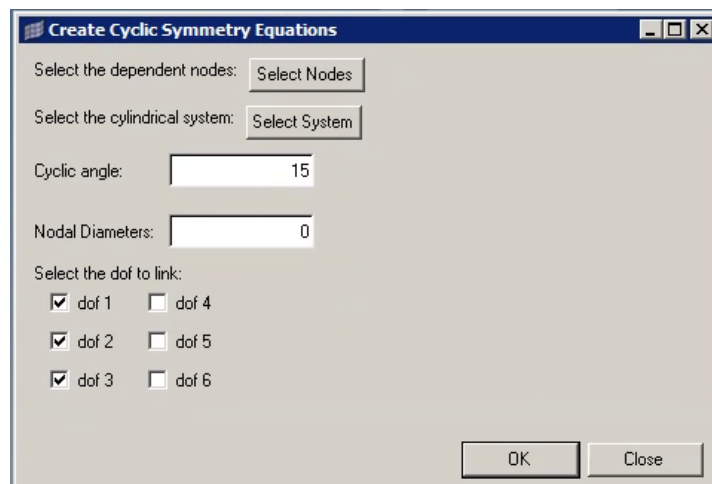
MPC	3	30000	1-1.0	20056	1-0.5	+
+		40056	1.8660254			

In this example we have decoupled the system of cyclic symmetry equations and applied them to the radial displacement (DOF = 1) of the nodes on the faces of the sector. The following image has been modified to have a more intuitive view of the nodal equations listed above.

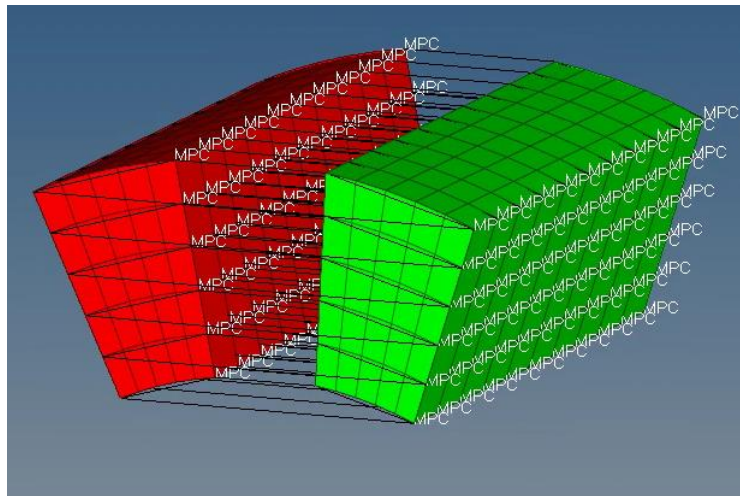


It's necessary repeat this operation for every node of the sector's faces in orders to achieve our purpose. For these reasons this procedure results too long to be handled manually, so it is necessary to develop an algorithm to automate the writing of all the equations for each DOF and for each nodal diameter of interest. It's possible do that by writing a macro function in a specific programming language supported by Hypermesh called the tcl/tk language.

In the next image is reported the graphical user interface (GUI) of the macro function. It writes the multi point constraint equations for each node by simply selecting the nodes on the basic sector's face and by setting the cyclic angle and the nodal diameter to analyze.



When the macro is launched all the MPC of the selected nodal diameter are defined and they appear as shown in the following picture:



Now that the equations have been implemented in the Optistruct environment, it is possible to validate the duplicate sector method by verifying that the analysis of the entire 360-degree model provides the same results as the analysis on the individual sector.

The validation of the method will be performed in two distinct phases. First, a modal analysis will be launched to verify that the natural frequencies of the whole component correspond to those of the cyclic symmetric sector.

If the analysis of the eigenvalues and the eigenvectors provides satisfactory results, we will proceed to a first topological optimization in order to verify that the solver optimizes the sector in the same way as the entire cylindrical structure.

The second phase of validation will focus on static analysis. We will apply a load case to the structure and verify that the displacements and stresses are consistent with those calculated by loading the model of the sector in the same way.

### 3.3.1 Modal analysis validation

In this section we will compare the results of the modal analysis obtained on the complete model with those obtained with the duplicate sector method. First of all it's necessary to set the modal analysis on the full 360° component. For these examples we chose to extract the first twenty not rigid modes and analyze their relative natural frequencies.

In the next picture is possible to understand how to set the load collector EIGRL in order to achieve our purposes. The EIGRL card defines data needed to perform real eigenvalue analysis (vibration or buckling) with the Lanczos Method. It's interesting to notice that the starting frequency of the modal analysis is set at  $\nu = 1$  Hz. This is the simplest way to avoid the first six rigid modes in the calculation, in fact they are usually located at very low frequencies, closer to the zero.



ANALYSIS RESULTS :

-----

ITERATION 0

(Scratch disk space usage for starting iteration = 6 MB)  
(Running in-core solution)

Volume = 3.90708E+06 Mass = 3.06706E-02

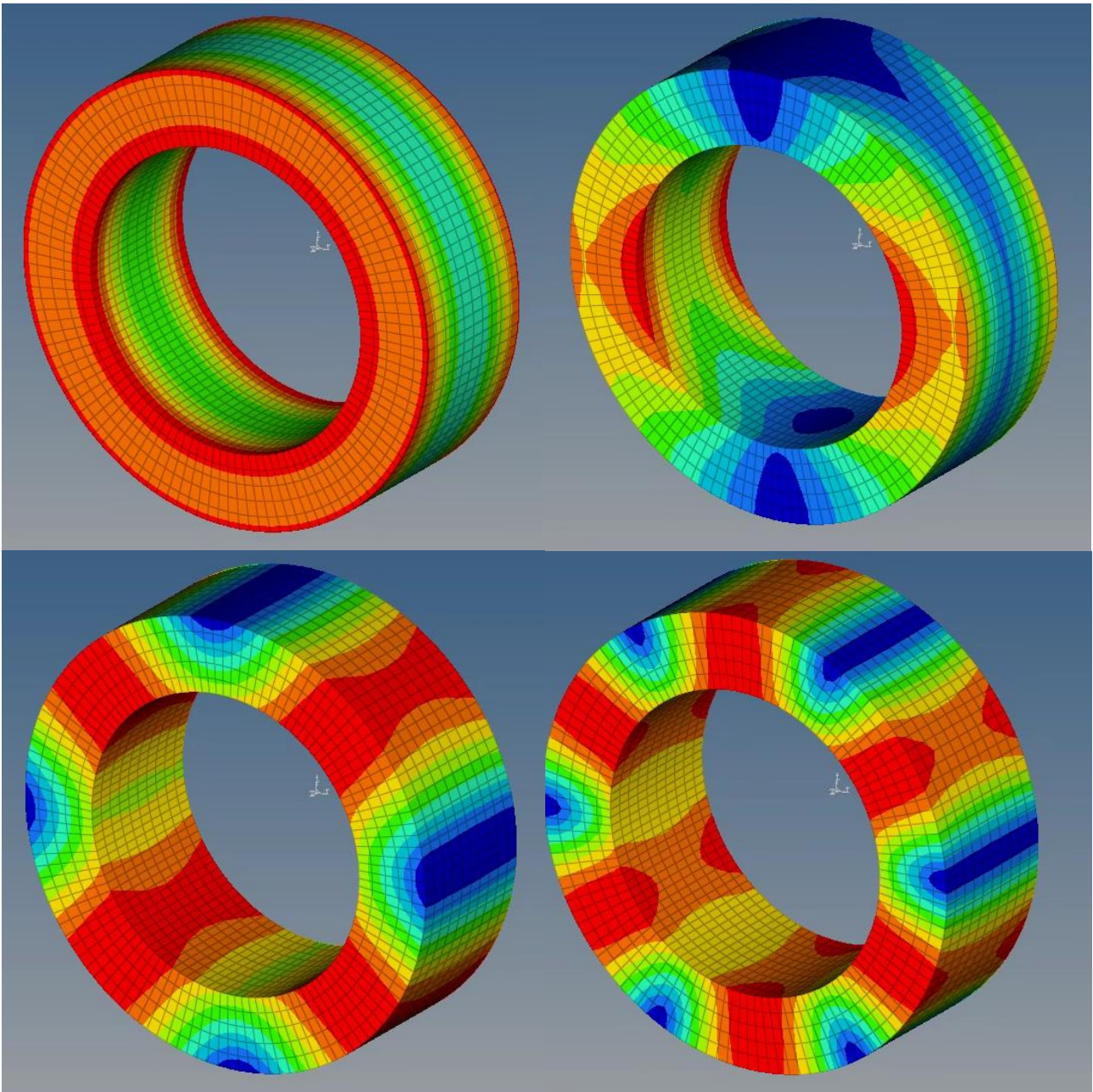
Subcase	Mode	Frequency	Eigenvalue	Generalized Stiffness	Generalized Mass
1	1	1.893324E+03	1.415173E+08	1.415173E+08	1.000000E+00
1	2	1.893324E+03	1.415173E+08	1.415173E+08	1.000000E+00
1	3	2.388690E+03	2.252576E+08	2.252576E+08	1.000000E+00
1	4	2.388690E+03	2.252576E+08	2.252576E+08	1.000000E+00
1	5	4.900740E+03	9.481632E+08	9.481632E+08	1.000000E+00
1	6	4.900740E+03	9.481632E+08	9.481632E+08	1.000000E+00
1	7	5.716167E+03	1.289940E+09	1.289940E+09	1.000000E+00
1	8	5.817464E+03	1.336064E+09	1.336064E+09	1.000000E+00
1	9	5.817464E+03	1.336064E+09	1.336064E+09	1.000000E+00
1	10	6.180525E+03	1.508032E+09	1.508032E+09	1.000000E+00
1	11	6.180525E+03	1.508032E+09	1.508032E+09	1.000000E+00
1	12	6.482340E+03	1.658912E+09	1.658912E+09	1.000000E+00
1	13	8.325131E+03	2.736162E+09	2.736162E+09	1.000000E+00
1	14	8.325131E+03	2.736162E+09	2.736162E+09	1.000000E+00
1	15	8.470337E+03	2.832443E+09	2.832443E+09	1.000000E+00
1	16	8.470337E+03	2.832443E+09	2.832443E+09	1.000000E+00
1	17	8.744854E+03	3.019012E+09	3.019012E+09	1.000000E+00
1	18	8.744854E+03	3.019012E+09	3.019012E+09	1.000000E+00
1	19	9.474755E+03	3.544017E+09	3.544017E+09	1.000000E+00
1	20	9.474755E+03	3.544017E+09	3.544017E+09	1.000000E+00

\*\*\*\*\*

ANALYSIS COMPLETED.

It's possible to visualize the deformed shape for each mode and so evaluate the eigenvectors (the nodal displacements) by uploading the output file to another Altair's tool: Hyperview.

Thanks to this platform we are able to visualize the nodal diameters of every normal modes. In the following images it's possible to see some examples of different nodal diameters, in the specific, they show four normal modes from  $ND = 0$  to  $ND = 3$ .



Once visualized all the twenty modes we can assign a specific nodal diameter to each of them. In this way we can proceed with the modal analysis of the sector. This case will be more laborious because we are forced to create more subcases as many as the nodal diameters involved.

After launched the solver (Optistruct) we are in presence of a first significative result. The next table shows the comparison in terms of normal frequencies. The results between the baseline and the sector are really similar in terms of percentage error and are completely the same in terms of harmonic index.

baseline-full 360°			duplicate sector method					% err
MODE	freq [Hz]	ND	H0[Hz]	H1[Hz]	H2[Hz]	H3[Hz]	H4[Hz]	
1	1.87E+03	2			1.87E+03			0.01
2	1.87E+03	2			1.87E+03			0.01
3	2.39E+03	2			2.39E+03			0.01
4	2.39E+03	2			2.39E+03			0.01
5	4.84E+03	3				4.84E+03		0.00
6	4.84E+03	3				4.84E+03		0.00
7	5.71E+03	0	5.71E+03					0.00
8	5.84E+03	3				5.84E+03		0.00
9	5.84E+03	3				5.84E+03		0.00
10	6.16E+03	1		6.16E+03				0.01
11	6.16E+03	1		6.16E+03				0.01
12	6.48E+03	0	6.48E+03					0.00
13	8.30E+03	2			8.30E+03			0.00
14	8.30E+03	2			8.30E+03			0.00
15	8.37E+03	4					8.37E+03	0.00
16	8.37E+03	4					8.37E+03	0.00
17	8.77E+03	1		8.78E+03				0.03
18	8.77E+03	1		8.78E+03				0.03
19	9.55E+03	4					9.55E+03	0.00
20	9.55E+03	4					9.55E+03	0.00

Satisfied by this first comparison it's time to proceed through the validation by confronting the eigenvalues and then the eigenvectors of the modal analysis. Let's start with the eigenvalues:

baseline-full 360°			duplicate sector method					% err	
MODE	freq [Hz]	ND	eigenvalue	H0	H1	H2	H3		H4
1	1.87E+03	2	1.38E+08			1.38E+08			0.00
2	1.87E+03	2	1.38E+08			1.38E+08			0.00
3	2.39E+03	2	2.26E+08			2.26E+08			0.00
4	2.39E+03	2	2.26E+08			2.26E+08			0.00
5	4.84E+03	3	9.23E+08				9.23E+08		0.00
6	4.84E+03	3	9.23E+08				9.23E+08		0.00
7	5.71E+03	0	1.29E+09	1.29E+09					0.00
8	5.84E+03	3	1.34E+09				1.34E+09		0.00
9	5.84E+03	3	1.34E+09				1.34E+09		0.00
10	6.16E+03	1	1.50E+09		1.50E+09				0.00
11	6.16E+03	1	1.50E+09		1.50E+09				0.00
12	6.48E+03	0	1.66E+09	1.66E+09					0.00
13	8.30E+03	2	2.72E+09			2.72E+09			0.00
14	8.30E+03	2	2.72E+09			2.72E+09			0.00
15	8.37E+03	4	2.76E+09					2.76E+09	0.00
16	8.37E+03	4	2.76E+09					2.76E+09	0.00
17	8.77E+03	1	3.04E+09		3.04E+09				0.00
18	8.77E+03	1	3.04E+09		3.04E+09				0.00
19	9.55E+03	4	3.60E+09					3.60E+09	0.00
20	9.55E+03	4	3.60E+09					3.60E+09	0.00

As we can see from the percentage error's column the results are absolutely coherent between the two models. Next step is the analysis and the comparison between the eigenvectors. As said before, the nodal displacements are normalized with the mass of the model, so the eigenvectors will be influenced by a scale

factor because of the difference in mass between the full 360° baseline and the sector model. In order to overcome this complication and obtain coherent results for the analysis it is therefore necessary to apply the following relation:

$$\{U_{360}\} = \frac{\{U_{sec}\}}{\sqrt{\frac{N}{2}}}$$

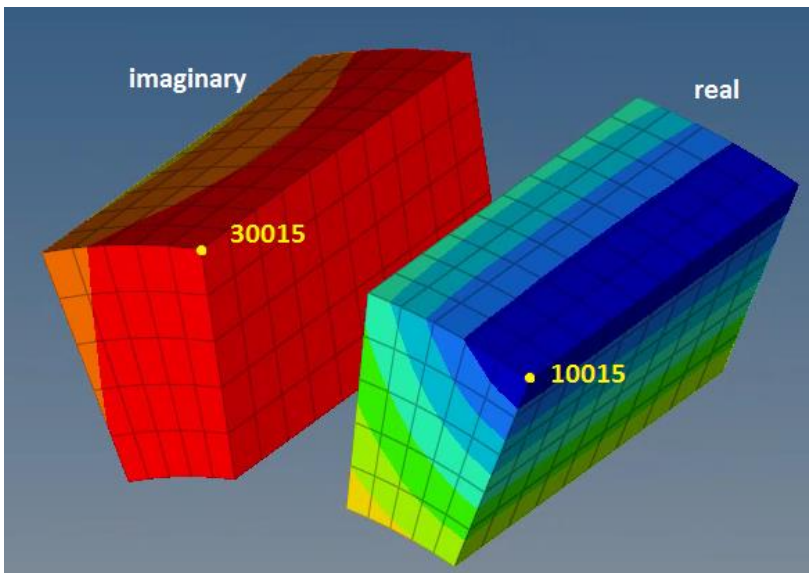
Where:

- $\{U_{360}\}$  is the displacements vector of the baseline;
- $\{U_{sec}\}$  is the displacements vector of the sector;
- $N$  is the numbers of sector; (in this case  $N = 24$ )

According to the duplicate sector method, which separates the real part from the imaginary one of the cyclic symmetry equations, the magnitude of the nodal displacements will be function of both these two components. It's therefore necessary to consider the displacement on the basic sectors nodes and those on the corresponding duplicated sector nodes. The resultant displacement's magnitude for each node  $i$  can be easily obtained with the following expression:

$$\{U_{sec}\} = \sqrt{\mathcal{R}_i^2 + \mathcal{I}_i^2}$$

Although the geometry in question is very simple, there are still too many nodes to report all the results in these pages. For this reason, we only report the calculation concerning a pair of nodes:



❖ **BASELINE 360**

Magnitude = 7.526;

❖ **SECTORS**

Real part: Node 10015

R = 1.03 e+01

Imaginary part: Node 30015

I = 2.40 e +01

Magnitude = 26.073

Scaled magnitude = 7.257;

❖ **ERROR = 0.01%**

The entire procedure was repeated for all the nodes and for each of the twenty normal modes. In all cases, the eigenvectors were consistent with the baseline and the percentage error never exceeded 0.05 %. In front of these results we can therefore conclude that the validation of the modal analysis is positively concluded. The dynamic part of the duplicated sector method works in the Optistruct environment. As mentioned before it's now possible launch our first topology optimization considering only the dynamic behavior of the component.

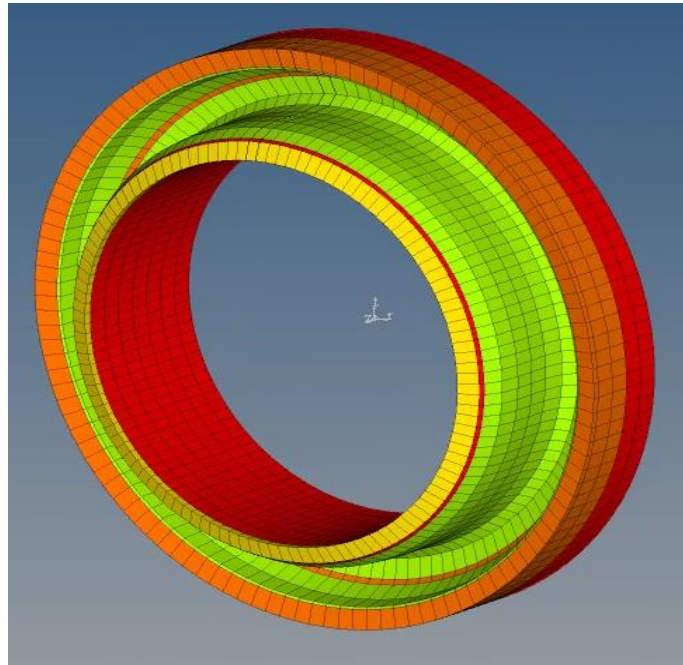
### 3.3.2 Dynamic topology optimization

In this section we will launch the optimizer for both the baseline and the individual sector to evaluate the final output. The optimization process starts from the definition of the objective function and the design constraints. For this first simple topology we chose the following parameter:

- OBJECTIVE: minimize volume;
- DESIGN SPACE: axial symmetry design space;
- MANUFACTURING CONSTRAINTS: no hole along the axial draw direction;
- DESIGN CONSTRAINTS: no first 2 modes between 1500 – 1877 Hz;

In addition to the design constraints and the objective it was considered the manufacturing constraint and the axial symmetry of the component. Notice that no static constraints like maximum displacements or stresses have been imposed to the optimization problem.

After creating the desired design responses (DRESP1) in the Hypermesh environment, we are ready to run Optistruct. Let's start with the baseline first as shown in the follow:



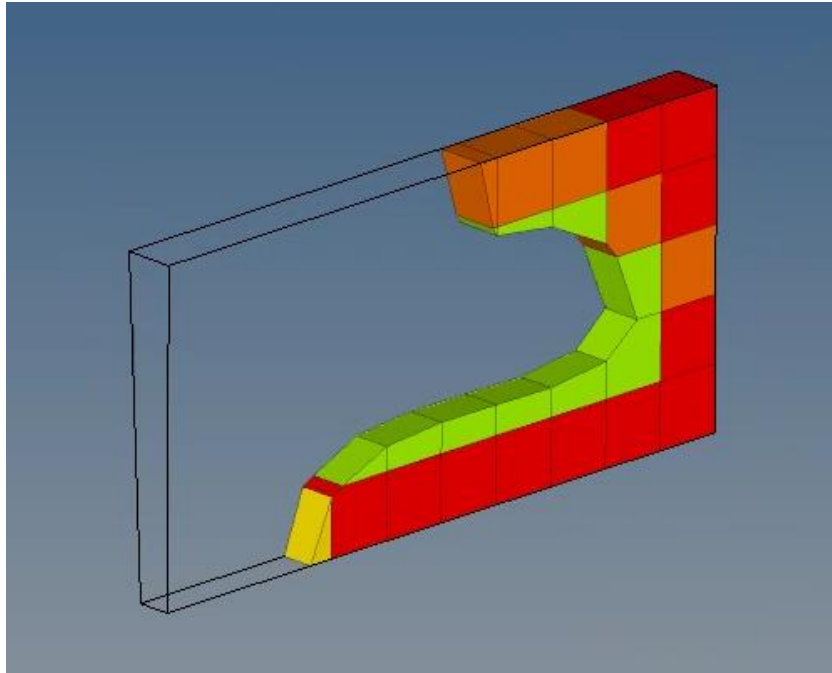
After 45 iterations the program reaches the results shown in the figure. As discussed in the chapter 2, the result is drastically influenced by the density index which can be set between zero and one. In this case it has been choose at 0.7 and of course it will be maintained the same in the following optimization of the sector. All the constraints are satisfied, we can check the frequency of the first two modes to verify that they are out of the range imposed in the pre-process phase:

```
Objective Function (Minimize VOLUM) = 2.02330E+06    % change =      -0.14
Maximum Constraint Violation %      = 0.66789E+00
Design Volume Fraction               = 5.15466E-01    Mass      = 1.58829E-02
```

Subcase	Mode	Frequency	Eigenvalue	Generalized Stiffness	Generalized Mass
1	1	1.489982E+03	8.764388E+07	8.764388E+07	1.000000E+00
1	2	1.489982E+03	8.764393E+07	8.764393E+07	1.000000E+00

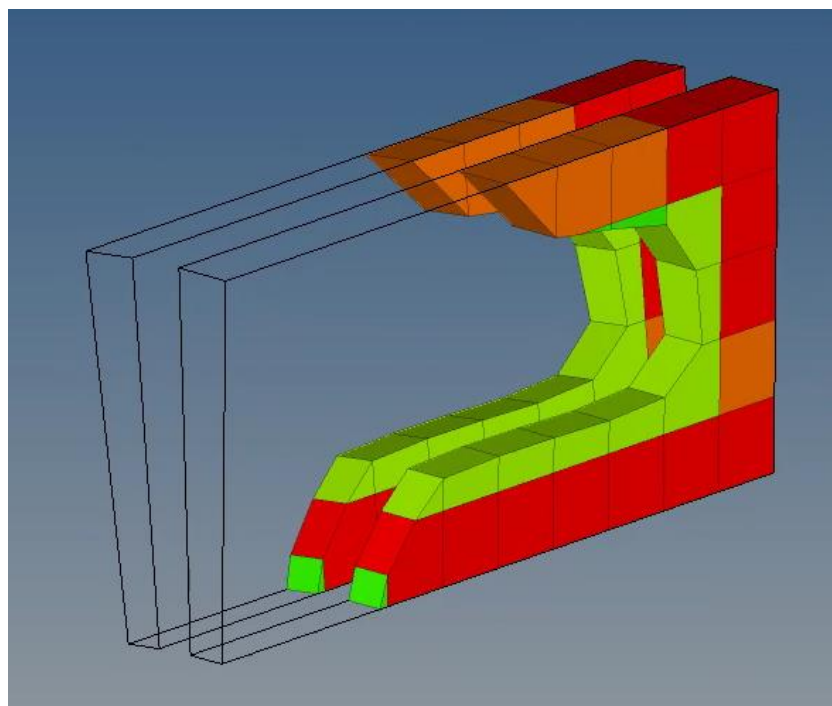
Those results are directly extracted from the output file, at the last iteration of the optimization process.

To better visualize the solution found by the solver a slice of the axisymmetric structure can be extracted from the solid. This will help us in the following comparison between this solution and that obtained with the duplicate sector method.



Speaking in terms of time, it's important to register that the CPU spends more than one minute to complete the process and precisely: 1'17".

Next step is the topology optimization of the cyclic symmetric sector. Settings are still the same but in addition, to implement axisymmetric, it needs to introduce one more feature on the design space. In the specific it is necessary to ensure that both the base and the duplicate sectors are optimized in the same way, with the same density distribution. The only way to implement this constraint in Optistruct is to define a master-slave pattern repetition relation between the two parts of the sector. The base sector will be the master while the duplicate sector's elements will be dependent from those of the basic sector.



In the figure above is reported the last iteration of the optimization process realized with the duplicate sector. The two sectors have the same density distribution for each element and this is the proof that the axisymmetric is effectively imposed thanks to the pattern repetition setting.

If compared, the two solutions are quite similar in the density distribution and in their general shape. The last topology optimization was completed after 38 iterations and only 3 seconds of CPU time. This means a time reduction of the 96 % respect to the optimization of the whole cylindrical model. This is of course the great advantage of the whole method: achieve the same result with great time savings.

Even in this case all the design constraints are satisfied, the frequency range of the first two modes is not violated and the volume has been minimized. The following image show an extract of the output file generated by the program.

```
Objective Function (Minimize VOLUM) = 3.39804E+04    % change =      0.14
Maximum Constraint Violation %      = 0.29405E+00
Design Volume Fraction               = 5.19420E-01    Mass      = 2.66746E-04
```

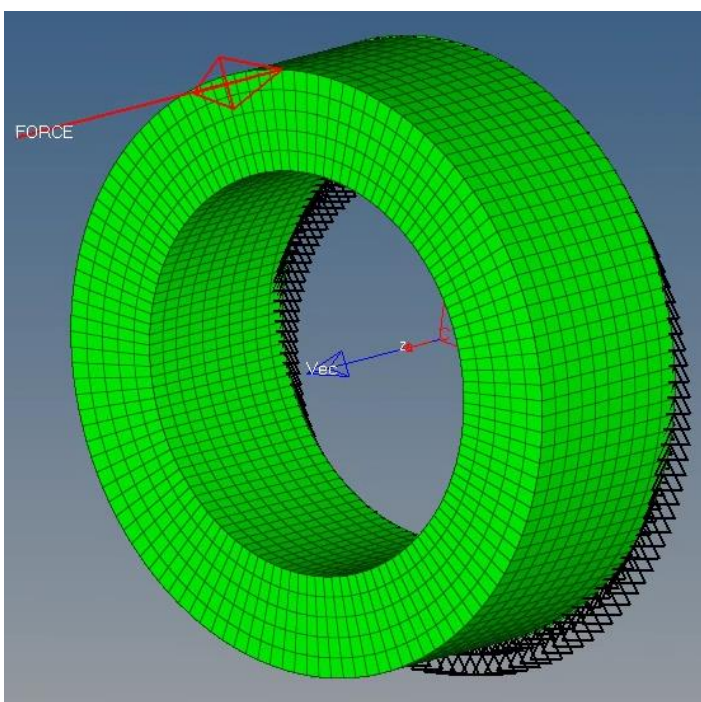
Subcase	Mode	Frequency	Eigenvalue	Generalized Stiffness	Generalized Mass
1	1	1.495589E+03	8.830483E+07	8.830483E+07	1.000000E+00
1	2	1.495593E+03	8.830526E+07	8.830526E+07	1.000000E+00

Thanks to this comparison and its relative results we can positively conclude this section with the affirmation that, dynamically speaking, the duplicate sector method's macro function is well implemented and it gives the expected advantages.

### 3.3.3 Static validation

The last step of the validation process consists in a simply linear static analysis. If the comparison between the solutions of the static analysis, that is to say the displacements of the full 360° structure and those of the sector, will be the same, then the duplicate sector method will be considered validated.

First, it must be defined a proper load case. In the gearbox analysis field, a force is usually applied to a single point of the model. To simulate this situation on the simple geometry object of the analysis it has been chosen the following load condition:



A force of arbitrary magnitude is applied in a single grid point. On the opposite surface of the model are located a set of constraints. In Hypermesh they are defined as single point constraints (SPC) and they are illustrated like triangles as shown in the figure beside. During this validation no DOFs will be left free on the constrained surface of the structure, so the single points constrained are defined to constraint all the six degrees of free.

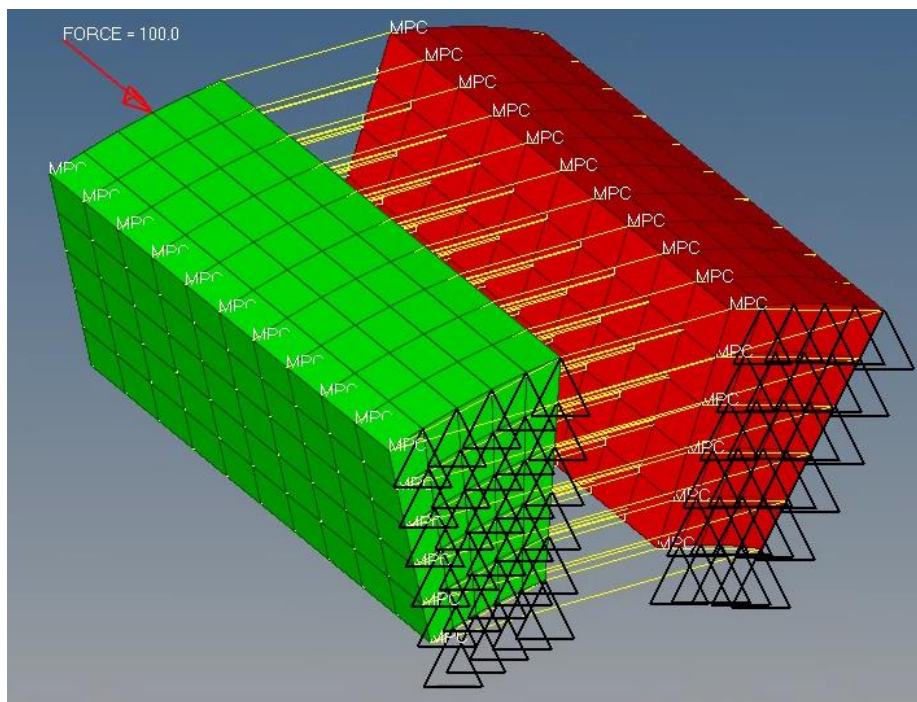
- Force magnitude: 100 N
- SPC DOFs: 1 2 3 [displacements]  
4 5 6 [rotations]

The following card image shows how to properly configure, in the Hypermesh/Optistruct environment, a linear static subcase with a load collector and a set of SPCs applied.

Load Collector (2)	SPCs	2	■
	Force	4	■
Load Step (1)	STATIC	2	
Name		Value	
Solver Keyword	SUBCASE		
Name	STATIC		
ID	2		
Include File	[Master Model]		
User Comments	Hide In Menu/Export		
<b>Subcase Definition</b>			
Analysis type	Linear Static		
SPC	SPCs (2)		
LOAD	Force (4)		

The load case definition has been repeated for the sector. In this case born the following question: “is it necessary a force applied only on the real part of the sector or on both the imaginary and real parts of it?” Actually this doubt remain opened because after a certain number of attempts, it seems that the result is not influenced at all by this fact but it returns the same solution both cases. Maybe the pattern repetition constraint and its master slave relation are responsible for this duality in the results.

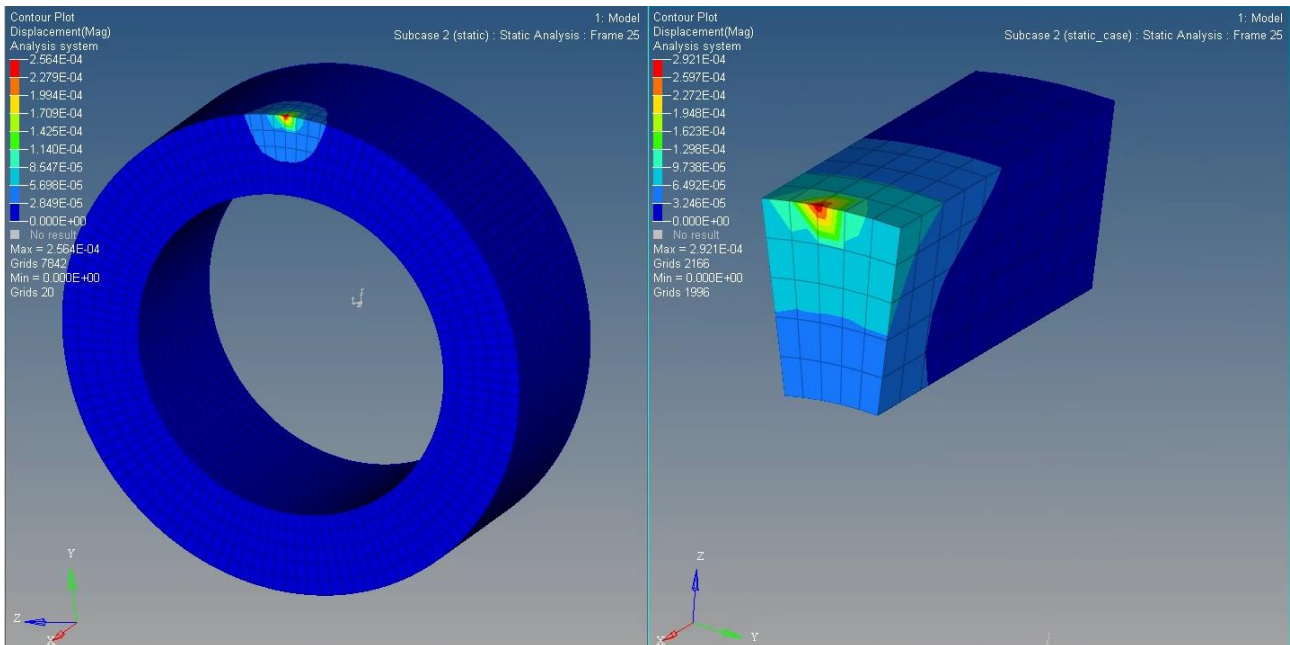
For this reason, it has been chosen to constraint both the sectors but apply the load only on the real part of it, that is to say the base sector. In the next picture is represented the static subcase applied to the model:



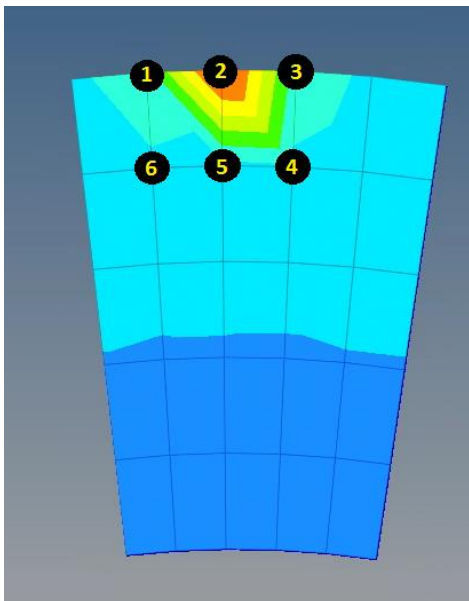
Again, it can be noticed the force applied in a single node of the basic sector’s mesh, and the SPCs applied on the opposite surface respect the load on both the sectors. About the yellow lines in the image above, it should be remembered that they are the multi point constraints representing the cyclic symmetry equations defined by the tcl/tk macro function implemented at the beginning of the present chapter.

It's important notice that the only cyclic symmetric equations to be implemented in a static analysis are those concerning the nodal diameter ND = 0 and not all the other harmonic indexes, considered instead during the previous modal analysis.

After running Optistruct, the results can be view through Hyperview. The following figure represents the most important and critical result achieved up to this point of this thesis work. It shows the comparison between the displacements of the two cases:



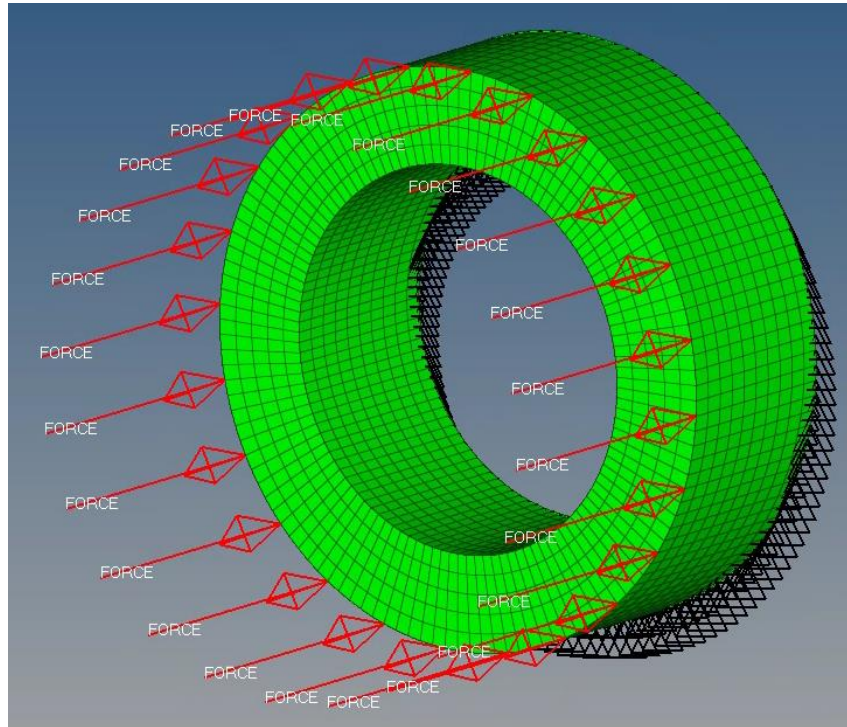
The solver finds two different solutions, both in terms of value and distribution of displacements. To better understand the problem, it's first necessary analyze the following list of results concerning the displacement of the six nodes around the point of force application as shown below:



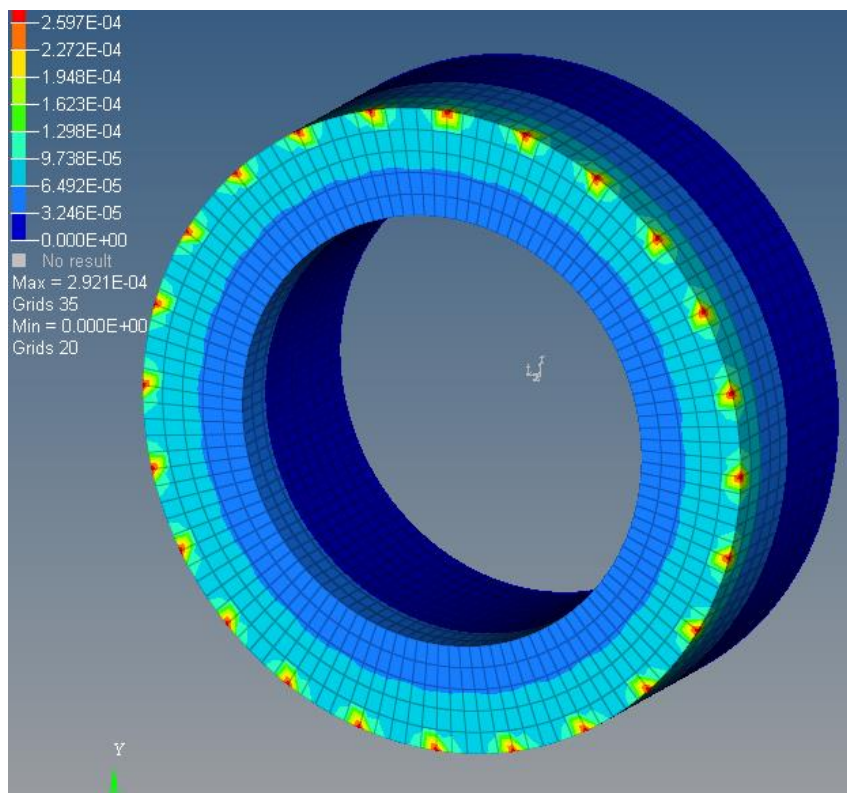
Node ID:	BASELINE FULL 360	DUPLICATE SECTOR METHOD
1	7.396 E-05	1.145 E-04
2	2.564 E-04	2.921 E-04
3	7.396 E-05	1.145 E-04
4	5.498 E-05	9.284 E-05
5	5.201 E-05	8.786 E-05
6	5.498 E-05	9.284 E-05

From the results analysis it's clear that the displacements are more intense in the case of the sector than those on the baseline. This is difficult to explain because the force is the same in both the cases but for some reason it appears higher on the sector.

After some hypothesis we found that the responsible of this strange behavior is the cyclic symmetric equations themselves. Once they are applied to the sector, every single node of the structure is not more only a node but it repeats itself N-time during the calculation. For this reason, a force applied at a node, actually acts like N forces repeated along the circumference. The next two figures better explain this concept:



To verify our last hypothesis, we need to run one more static analysis on the baseline model where the force is repeated 24 times. This time the displacements comparison leaves no doubt:



As shown in the figure above, it is evident that the displacements calculated by the duplicate sector method are the result of the loads' superposition acting on the adjacent sectors.

### **3.3.4 Conclusions on the duplicate sector method**

After several attempts to fix the problem encountered during the static analysis we have come to the following conclusion: despite the positive results of the modal analysis and the relative topological optimization, the duplicate sector method cannot be considered valid. The impossibility of applying a non-cyclic symmetric load to a single sector has forced to leave the idea of optimizing cyclic symmetric structures considering only a sector.

In the hope that future versions of the software will implement this possibility, we will continue this thesis work with the optimization of the whole 360° component of the test case in question: the pinion of the transfer gear box mounted on the GE 9X turbofan as illustrated in the next chapter.

## **4. Test Case**